

# COMPARATIVE STUDY OF THE PERFORMANCE OF FLAT SOLAR PANELS

Malahimi ANJORIN<sup>1</sup>, Christophe AWANTO<sup>1</sup>, Aristide C. HOUNGAN<sup>1</sup>, Donald K. T. DEDO<sup>1</sup>, Michel FEIDT<sup>2</sup>

<sup>1</sup>LEMA-EPAC, University of Abomey-Calavi, 01 BP 2009 Cotonou Benin.

<sup>2</sup>LEMTA-CNRS 875-2 Ave. of Haye Forest, BP 160-54504 Vandoeuvre France

## ABSTRACT

In a context where the price of fossil fuels keeps on rising and the environment continues to deteriorate, energy saving is a priority. Faced with this situation, man is interested in renewable energy sources first and foremost solar energy. This article presents one of the applications of solar energy. It is about the production of hot sanitary water by a solar water heater. Six types of plane solar panels have been studied. This study lies within a perspective of comparing performance of these different types of sensors, focusing on the development and use of simulation tools. MATLAB simulation was used to compare the performance of different solar panels. The plotted curves show that the performance increases with the mass flow of the coolant, whereas the outlet temperature of the fluid goes down at the same rate.

**Keywords:** *Plane solar panels, performance, coolant, simulation, energy saving*

## 1 INTRODUCTION

Soaring oil costs and enormous environmental problems caused by the combustion of hydrocarbons whose supply may be random, are currently at the heart of global concerns. Energy, in all its forms (electrical, thermal, etc...) becomes increasingly inaccessible to a group of people or regions for which no alternative solution at lower cost is considered. To cope with this situation, renewable energy sources are now the only use to which the world turns, especially the industrial world to overcome the problems of pollution, depletion of natural energy resources that dry up.

Indeed, some hotels in Cotonou (the economic capital), produce sanitary hot water by the joint action of desuperheaters (heat exchangers) of chillers and resistors. The use of these electric heaters, energy-intensive a priori to be more expensive in the long run than heating water from solar energy which is an inexhaustible source, free and available [2]. Moreover, the conversion of solar energy into heat for the hot water must be through a solar water heater made of plane panel, piping and storage tank of hot water.

Several studies and achievements of solar water heaters exist worldwide. The characteristic often used, is performance. FEIDT and al. [3] expressed the instantaneous efficiency of a flat panel according to a coefficient  $F_R$  which is equal to the amount of heat actually derived based on the amount of heat removed if the absorber were at the fluid temperature.

The current study, after introducing the system by specifying the different types of sensors studied, modeled it by physical equations that are programmed. Finally, the overall performance of the sensors studied is compared through a simulation of their continuous operation.

## 2 VARIOUS CATEGORIES OF SOLAR PANELS STUDIED AND SIZING

### 2.1 The different categories of sensors studied

The plane solar panel, sometimes called insulator, is the link between incoming solar energy and the consumer. It is a device which captures on a surface, generally planar and fixed, the direct and diffuse radiation which is immediately absorbed and converted into heat.

#### 2.1.1. Sensor type 1

The absorber is in plate and the water circuit consists of circular tubes. This technique is generally the most used. It is to be welded on a metal plate a number of parallel tubes with a constant spacing between 5 and 15 cm depending on the models. These tubes are connected at the top and bottom by two manifolds not shown in the pictures. The fluid inlet is at the bottom and the outlet on the opposite side, at the top in order to ensure the same flow to each tube.

The heat produced in the plate acting as a heating blade with respect to the tube is transferred transversely to the tube and as a result, heating the fluid by convection. The tube earns a flux directly captured on its outer diameter assumed at a uniform temperature.

#### 2.1.2. Sensor type 2

The absorber is plate and the water circuit consisted of plates. In this case, the absorber is only consisting of a flat plate. Water flows between that plate and another one is placed a few millimeters below the absorption plate. These two plates lead on both sides of the inlet and outlet manifolds, not shown in Picture 2.

#### 2.1.3. Sensor type 3

The absorber is wavy. It is similar to the sensor of type 1.

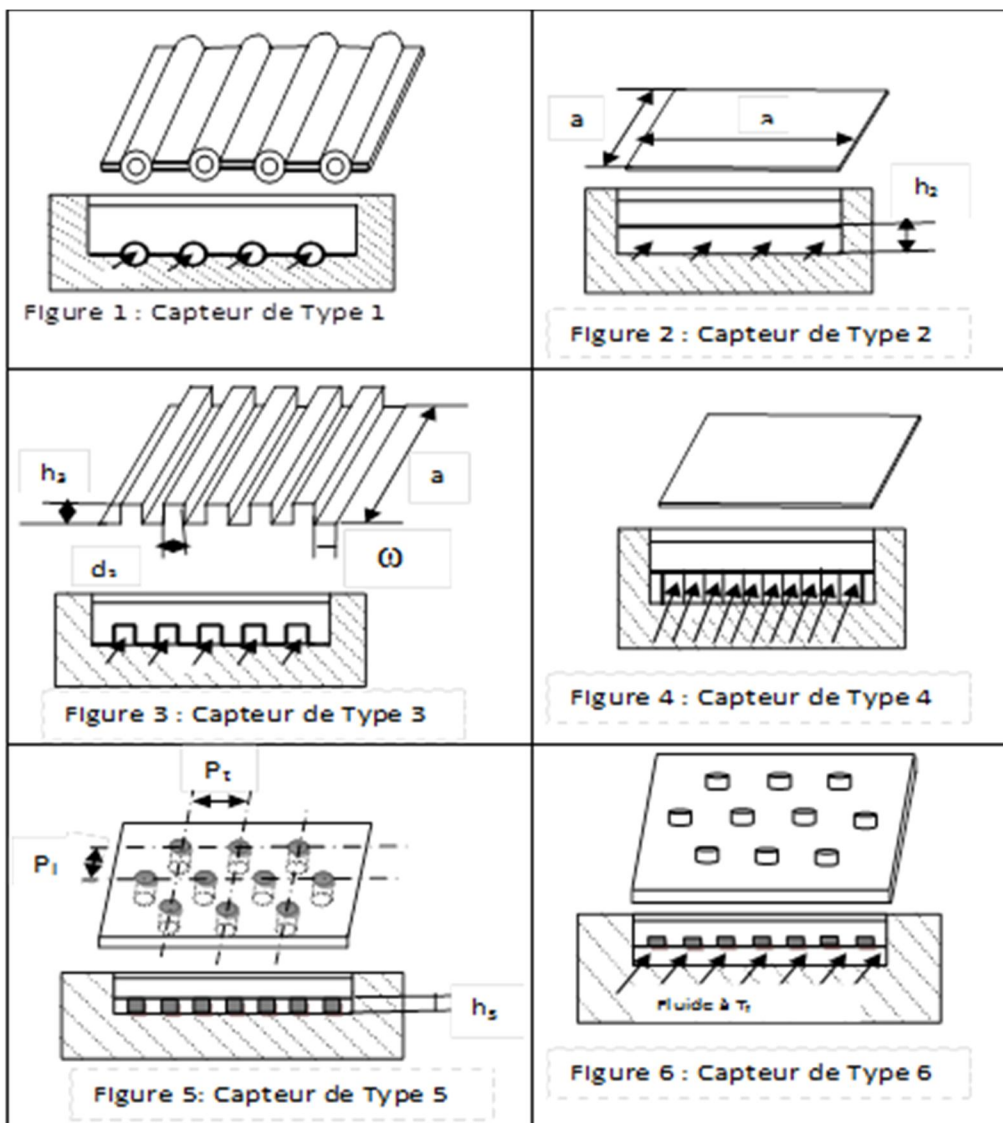


Table 1: Sizes of the different types of sensors

different types of sensors	Dimensions
Type 1	$n_{\text{tubes}} = 17$ ; $\omega = 21 \text{ mm}$ ; $S_1 = 1,5 \text{ m}^2$ ; $D_1 = 44 \text{ mm}$
Type 2	$h_2 = 3 \text{ mm}$ ; $a = 1000 \text{ mm}$ ; $S_2 = 1 \text{ m}^2$ ; $D_2 = 44 \text{ mm}$
Type 3	$h_3 = 12 \text{ mm}$ ; $S_3 = 1,36 \text{ m}^2$ ; $D_3 = 44 \text{ mm}$
Type 4	$h_4 = 3 \text{ mm}$ ; $a = 1000 \text{ mm}$ ; $S_4 = 1,1 \text{ m}^2$ ; $D_4 = 44 \text{ mm}$
Type 5	$h_5 = 3 \text{ mm}$ ; $n = 574 \text{ trous}$ ; $D = 4 \text{ mm}$ ; $P_t = 48 \text{ mm}$ ; $P_1 = 28 \text{ mm}$ ; $S_5 = 1,02 \text{ m}^2$ ; $D_5 = 44 \text{ mm}$
Type 6	$h_6 = 3 \text{ mm}$ ; $n = 574 \text{ trous}$ ; $D = 4 \text{ mm}$ ; $P_t = 48 \text{ mm}$ ; $P_1 = 28 \text{ mm}$ ; $S_6 = 1,02 \text{ m}^2$ ; $D_6 = 44 \text{ mm}$

Here, the absorber is in the form of waves. Water flows in this case, between a flat plate based on the insulator and the upper surface of the corrugated absorber (see Picture 3). The lower surface of the absorber acts as heating fin relative to the rectangular tube formed by the waves. This tube receives then the solar flux directly captured over its width and that trans-

ferred by the blades. Only the coolant channels lead directly to inlet and outlet manifolds not shown.

#### 2.1.4. Sensor type 4

The absorber is plate and the water circuit consists of plates

and waves. This is the schema of type 2 to which we add waves in the coolant circuit as shown in Picture 4.

### 2.1.5. Sensor type 5

The flat plate absorber is provided with small circular holes not opening. It has the same configuration as the sensor type 2. We carry on its absorber holes that do not lead to the coolant circuit. These holes are made so that bumps are formed and placed on the second sheet of the coolant circuit (Picture 5). The holes can be arranged in line or staggered. The thermal point of view, the staggered arrangement provides a higher heat transfer coefficient because of better mixing of the fluid. But in return, the losses are increased. For the present study, this provision has been chosen, because of its thermal advantages on the online disposal.

### 2.1.6. Sensor type 6

The absorber is equipped with flat plate and provided with small circular holes not leading, but the non-leading parts are directed to the sky. It is similar to the previous case, except that the absorber is reversed compared to type 5. In this case, the surface provided with bumps is oriented towards the sky (Picture 6). The pitch in types 3, 5 and 6 should be selected so that the incident solar energy is trapped in the troughs. It is then formed on the surface small black bodies that can increase the energy captured.

## 2.2. Sizing the system

To determine the dimensions of the essential elements of different types of sensors, we make the following considerations: the different organs of sensors will be sized relative to the sensor plate on a surface capture of  $1 \times 1 \text{m}^2$ . Thus, we choose a square surface shape of 1 m side; and the flow section of the coolant is the same for all types of sensors. Considering these assumptions, we'll determine the dimensions of the essential elements of the sensor type 2 and from these dimensions, we will then determine those of other types of sensors.

For technical and availability reasons, the height of the waves of heat exchangers is generally between 3 and 12 mm and for fear of piercing the surface of the absorber of sensors types 5 and 6, the holes made in the absorber must have an optimum height. We take  $h_2$  lowest possible. We hence choose  $h_2 = 3 \text{ mm}$ . So the passage section gives:  $s_2 = 3 \times 1000 = 3.10^3 \text{ mm}^2$ .

The calculation of the diameter  $D_2$  of the manifold is obtained from the equation of flow conservation:

$$Q = q \Rightarrow (\pi D^2 V) / 4 = v \cdot S_2 \\ \text{We assume } V = 2v. \text{ Thus, we have:}$$

$$\frac{\pi}{2} D_2^2 V = s_2 = a h_2 \Rightarrow D_2 = \sqrt{\frac{2ah_2}{\pi}} = \sqrt{\frac{2 \times 1000 \times 3}{\pi}} \approx 44 \text{mm} \quad (1)$$

Table 1 in page n°1 of this paper shows the sizes of the different types of sensors studied.

## 3 MODELLING THE SENSOR OPERATION

### 3.1. Heat balance on the plane sensor

The heat balance of the plane solar panel is based on the following reasoning: during operation time  $dt$ , the sensor receives an incident solar energy  $S_{G(i,\gamma)} \cdot dt$  and absorbs  $\varphi_{sa} \cdot dt$ . But this energy is not used entirely for heating the fluid, the sensor being the seat of heat loss, hot surfaces exchange heat with the environment by radiation and convection. In addition, a portion ( $E_c$ ) of the energy is stored in the sensor and expressed the thermal inertia in the unit. The law of conservation of energy gives:

$$\begin{aligned} \varphi_{sa} \cdot dt &= \varphi_u \cdot dt + \varphi_p \cdot dt + dE_c \\ \varphi_{sa} &= \varphi_u + \varphi_p + \frac{dE_c}{dt} \end{aligned} \quad (2)$$

In permanent mode of operation, the energy  $E_c$  stored in the sensor remains constant. The variation of this energy with respect to time is therefore nil:  $dE_c/dt = 0$  and equation (2) becomes:

$$\frac{dE_c}{dt} = 0 \text{ et l'équation (2) devient :} \\ \varphi_{sa} = \varphi_u + \varphi_p \quad (3)$$

### 3.2. Expressing $\varphi_{sa}$ and $\varphi_u$

The power absorbed by the sensor is written as follows:

$$\varphi_{sa} = \tau_{cs} \alpha_{ps} G_{(i,\gamma)} \cdot S \quad (4)$$

In the case of the flat panels, the coolant does not undergo a change of state. In this case, the useful flux can be written as:

$$\dot{\varphi}_u = m_f c_p (T_{fs} - T_{fe}) \quad (5)$$

The useful flux can also be written as a function of the thermal efficiency ( $F'$ ) of the sensor and the heat extraction factor ( $F_R$ ) by:

$$\varphi_u = S \cdot F' [\tau_{cs} \cdot \alpha_{ps} G_{(i,\gamma)} - h_p (T - T_a)] \quad (6)$$

where  $F$  is the factor (optical) efficiency with:

$F = 1$  for  $T = T_{pm}$  (average temperature of the absorber);  $F = F'$  for  $T = T_{fm}$  (mean fluid temperature) for  $F = F_R$  for  $T = T_{fe}$  (inlet temperature of the fluid);  $h_p$  is the overall surface conductance of heat losses.

The thermal efficiency of the absorber and the heat extraction factor are defined by [4]:

$$h_{c,c-a} = h_{vent} = 5,7 + 3,8 u_{vent} \quad (\text{W/m}^2\text{K}) \quad [5]$$

$$F' = \frac{1}{L \left[ \frac{1}{(D+2\omega\eta_a)h_p} + \frac{1}{(2D+2d)h_i} \right]} \quad (7)$$

$$F_R = \frac{q_{tf}}{h_p} \left[ 1 - \exp \left( -\frac{F' h_p}{q_{tf}} \right) \right] \quad (8)$$

They are based on  $h_p$ ,  $h_i$ ,  $\eta_a$  and geometry. It is then possible to express the flux  $\square_u$  according to  $F_R$ . This expression  $\varphi_u$  is very convenient, because it only depends on the input parameters and on the designing of the solar manifold.

$$\varphi_u = SF_R [\varphi_{sa} - h_p(T_{fe} - T_a)] \quad (9)$$

### 3.3. Expressing losses $\varphi_p$

Heat losses from the sensor are put in the form:

$$\varphi_p = h_p (T_{pm} - T_a) S \quad (10)$$

In the case of a flat solar panel, the average temperature of the absorbent wall  $T_{pm}$  evolves between the arithmetic mean of inlet, output temperatures, and the temperature of the fluid at the outlet of the device. Given the temperature difference  $\Delta T$  between the fluid and the absorbent wall, we have:

$$T_{pm} = \frac{T_{fs} + T_{fe}}{2} + \Delta T$$

$$T_{pm} = \frac{3T_{fs} + T_{fe}}{4} + \Delta T \quad (11)$$

$$h_p = \frac{1}{\frac{1}{h_{c,p-c} + h_{r,p-c}} + \frac{1}{h_{vent} + h_{r,c-a}}} +$$

$$+ \frac{1}{\frac{1}{h_{c,p-b} + h_{r,p-b}} + \frac{\epsilon_i}{\lambda_i} + \frac{1}{h_{vent}}} \quad (12)$$

where  $h_{r,p-c}$ ,  $h_{vent}$ ,  $h_{r,c-a}$ ,  $h_{r,p-b}$  are respectively the coefficients of the radiation between absorbent and transparent cover wall, the convection coefficient between the sensor and the external environment, radiation coefficient between cover and the external environment and radiation coefficient between absorbent wall and bottom of the sensor in  $\text{W/m}^2\text{K}$  calculable by the formulas:

$$h_{r,p-c} = \sigma \frac{(T_{pm}^2 + T_{cm}^2)(T_{pm} + T_{cm})}{\frac{1}{\epsilon_p} + \frac{1}{\epsilon_c} - 1} \quad (13)$$

$$h_{r,c-a} = \sigma \cdot \epsilon_c \frac{T_{cm}^4 - \epsilon_a T_a^4}{T_{cm} - T_a} \quad (15)$$

$$h_{r,p-b} = \sigma \frac{(T_{pm}^2 + T_{bm}^2)(T_{pm} + T_{bm})}{\frac{1}{\epsilon_p} + \frac{1}{\epsilon_b} - 1} \quad (16)$$

$h_{c,p-c}$  et  $h_{r,p-b}$  are obtained by equation below [6] :

$$Nu = 1 + 1,44 \left( 1 - \frac{1708}{Gr \Pr \cos j} \right) \left[ 1 - \frac{1708(\sin(1,8)^{1,6})}{Gr \Pr \cos j} \right] + \left[ \left( \frac{Gr \Pr \cos j}{5830} \right)^{\frac{1}{3}} - 1 \right] \quad (17)$$

For an angle of inclination of the sensor between 0 and  $\varphi^*$  with  $\varphi^* = \tan^{-1}(4800 \Pr)$ .

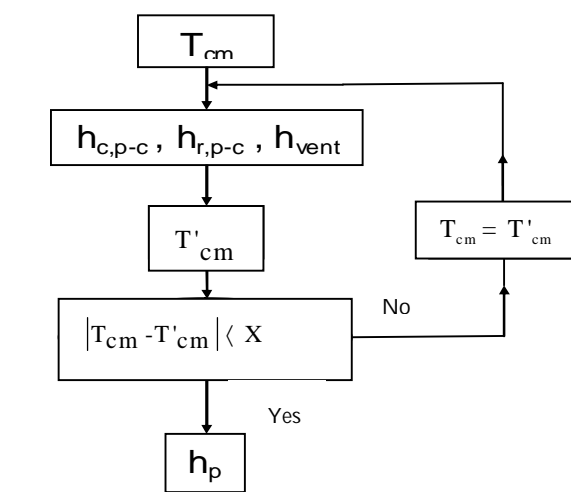
### 3.4. Determining the temperature of the glass plate $T_{cm}$

In dynamic stationary operation mode, the flux of heat loss between  $T_p$  and  $T_c$ , then  $T_c$  and  $T_a$  are identical. This enables to write the thermal balance of the transparent cover as follows:  $h_{c,p-c} + h_{r,p-c}(T_{pm} - T_{cm})S = (h_{vent} + h_{r,c-a})(T_{cm} - T_a)S$   $(18)$

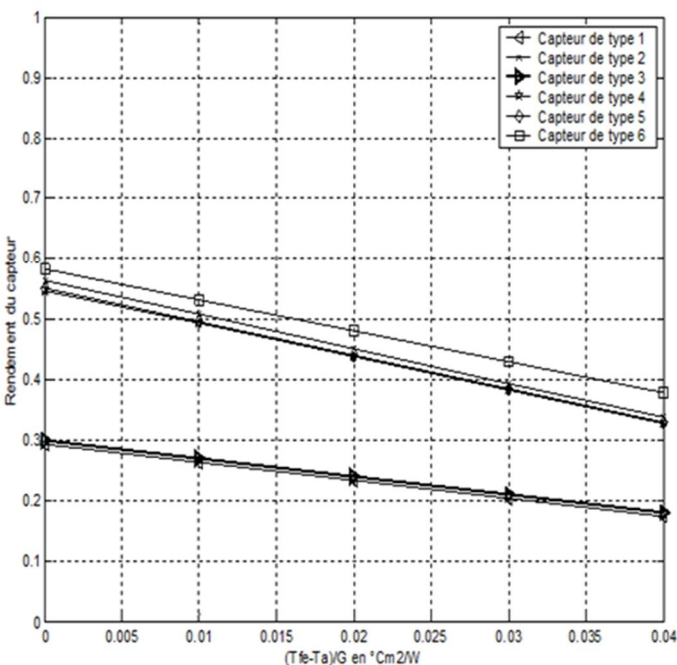
Knowing  $T_{pm}$  allows to calculate  $T_{cm}$  by solving equation (18) by an iterative method. According to this equation, we have:

$$T_{cm} = \frac{(h_{c,p-c} + h_{r,p-c})T_{pm} + (h_{vent} + h_{r,c-a})T_a}{(h_{c,p-c} + h_{r,p-c}) + (h_{vent} + h_{r,c-a})} \quad (19)$$

$h_{c,p-c}$ ,  $h_{r,p-c}$ , and  $h_{r,c-a}$  being functions of  $T_{cm}$ , formula (19) helps to find out  $T_{cm}$  by iterations. The algorithm expressing this iterative calculation is shown in Picture 7



Picture 7: Flowchart for calculating the temperature of the glass plate



Picture 8 : Change in overall performance based on the ratio

$$T^* = (T_{fe} - T_a)/G(i, \gamma)$$

### 3.5. Performance of the solar panel

The performance of a panel is defined compared to the incident solar flux as follows [7]:  
Overall performance: It is defined by:

$$\eta = \frac{\Phi_u}{G(i, \gamma) S} = F_R \left[ \frac{\varphi_{sa} - h_p (T_{fe} - T_a)}{G(i, \gamma)} \right] = F_R \left[ \eta_0 - \frac{h_p (T_{fe} - T_a)}{G(i, \gamma)} \right] \quad (20)$$

$$\text{Internal performance } \eta_i = \frac{\Phi_u}{\Phi_{sa}} \quad (21)$$

optical efficiency

$$\eta_o = \frac{\Phi_{sa}}{G(i, \gamma) S} = \frac{\tau_{cs} \alpha_{ps} G(i, \gamma) S}{G(i, \gamma) S} = \tau_{cs} \alpha_{ps} \quad (22)$$

## 4 SIMULATION OF THE SENSORS EFFICIENCY AND COMPARISON OF PERFORMANCE

In this part of the comparative study of the performance, the equations of the system as modeled and quite complex, the transition to programming has been helpful. For this, a software has been chosen to program the equations, and then determine and simulate the performance of the sensor before analyzing the re-

sults. To do this, several programming languages are available. We opt for "MATLAB" software.  
The assumptions for this study are:

The sensors are under stationary dynamic operation mode. They will be made with the same materials. But the geometry or shape of the absorber varies from one sensor to another, they operate under the same climate conditions assumed to be constant over the entire study period (we take the same global solar flux density  $G(i, \gamma)$ , the same ambient temperature  $T_a$  for all sensors); the initial temperature of the fluid is assumed to be the same for all sensors.

Under these conditions, the optical performance is the same for all types of sensors. Equation (19) of the general expression for the performance of a sensor shows us that it is increasing in  $F_R$  and decreasing in  $h_p$ . To capture the maximum energy, the sensor must be inclined at an angle equal to the latitude of the place [8]. But to avoid stagnation of water on the sensor, we take an inclination angle of  $10^\circ$  when the latitude of the place is less than this value, which was the case for this study. Picture 8 shows that the overall performance flat sensors fall when  $T^*$  increases, that is to say, for an illumination  $G(i, \gamma)$ , for example, the performance decrease when the temperature difference between the fluid and the ambient environment increases. This shows that the sensors performance is better at low temperatures, for they operate with less heat loss.

## 5 CONCLUSION

Six types of sensors have been studied in this work. After describing the system, a formal equation for various complex phenomena is performed. Then these equations were programmed using the software "MATLAB". This allowed to compare different performance by simulating the operation of the system.

The simulation of the operation helps to identify three groups of sensors including :

- Group 1 (corrugated absorber or finned) sensors 1 and 3
- Group 2 (flat absorber) sensors 2 and 4
- Group 3 (flat absorber with holes): sensors 5 and 6

It has been shown that the sensors belonging to group 1 have a lower performance than the ones of the other groups. Sensors in groups 2 and 3 have approximately equal performance. Holes made on the surface of the absorber of sensor 2 (types 5 and 6) have not a great influence on the performance of this sensor. In a nutshell, we conclude that the sensors operating at lower temperatures are more efficient since they operate with less heat loss. For this reason, the solar installation should always be made so as to allow the operating temperature of the sensors as low as possible.

## REFERENCES

- [1] DEDO D. K. Comparative study of flat solar panels, Dissertation for Engineering Design Degree (DIC), EPAC / UAC, Abomey-Calavi, pp. 135 (2008).
- [2] DUFFIE J. A., BECKHAM W.A., Solar engineering of thermal processes, John Wiley and Sons, New York, pp. 160-325, (1980).
- [3] FEIDT M., COSTEA M., BOUSSEHAIN R., PETRE C., Energy Engineering applied to solar - Solar Thermal Energy, Bucharest, p. 39-54 (2004).
- [4] LELEU R., Design and technology of thermal systems, Lavoisier, pp. 136-137, (2002).
- [5] AWANTO C., Technical aspects of pre-feasibility studies of solar projects: methodological approach of systems sizing, December, pp. 21-23(2003).
- [6] JANNOT Y., Solar Thermal, <http://www.google.com>, accessed 7th March 2008, p. 33-59, (2007).
- [7] DEGLA A.E., HOUDJOHON J. E., Study and design of a prototype solar flat water heater, Dissertation for Civil Engineering Degree (DIT), EPAC / UAC, Abomey-Calavi, pp. 9-62 (1998).
- [8] SEVO B.N., Identification of parameters of thermal efficiency of a solar parabolic trough, Dissertation for Comprehensive Study Diploma (DEA), EPAC / UAC, Abomey-Calavi, December, p59 - 63, (2001).